

Learning to learn ecosystems from limited data - a meta-learning approach

Zheng-Meng Zhai,¹ Bryan Glaz,² Mulugeta Haile,³ and Ying-Cheng Lai^{1,4,*}

¹*School of Electrical, Computer and Energy Engineering,
Arizona State University, Tempe, AZ 85287, USA*

²*Vehicle Technology Directorate, CCDC Army Research Laboratory,
2800 Powder Mill Road, Adelphi, MD 20783-1138, USA*

³*Vehicle Technology Directorate, CCDC Army Research Laboratory,
6340 Rodman Road, Aberdeen Proving Ground, MD 21005-5069, USA*

⁴*Department of Physics, Arizona State University, Tempe, Arizona 85287, USA*

(Dated: October 11, 2024)

A fundamental challenge in developing data-driven approaches to ecological systems for tasks such as state estimation and prediction is the paucity of the observational or measurement data. For example, modern machine-learning techniques such as deep learning or reservoir computing typically require a large quantity of data. Leveraging synthetic data from paradigmatic nonlinear but non-ecological dynamical systems, we develop a meta-learning framework with time-delayed feedforward neural networks to predict the long-term behaviors of ecological systems as characterized by their attractors. We show that the framework is capable of accurately reconstructing the “dynamical climate” of the ecological system with limited data. Three benchmark population models in ecology, namely the Hastings-Powell model, a three-species food chain, and the Lotka-Volterra system, are used to demonstrate the performance of the meta-learning based prediction framework. In all cases, enhanced accuracy and robustness are achieved using five to seven times less training data as compared with the corresponding machine-learning method trained solely from the ecosystem data. A number of issues affecting the prediction performance are addressed.

I. INTRODUCTION

Recent years have witnessed a growing interest in applying machine learning to complex and nonlinear dynamical systems for tasks such as prediction [1–25], control [26], signal detection [27], and estimation [28]. For example, a seminal work [5] exploited reservoir computing [29, 30] to accurately predict the state evolution of a spatiotemporal chaotic system for about half dozen Lyapunov times (one Lyapunov time is the time needed for an infinitesimal error to grow by the factor of e) - a remarkable achievement considering the sensitivity of a chaotic system to uncertainties in the initial conditions). Subsequently, long-term prediction of chaotic systems with infrequent state updates was achieved [12], and a parameter-adaptive reservoir computing was developed to predict critical transitions in chaotic systems based on historical data [16, 23].

The demonstrated power of modern machine learning in solving challenging problems in nonlinear dynamics and complex systems naturally suggest applications to ecological systems that are vital to the well being of the humanity. Ecosystems in the modern era are nonautonomous in general due to the human-influences-caused climate change, and it is of paramount interest to be able to predict the future state of the ecosystems. However, to enable applications of machine learning to ecosystems, a fundamental obstacle must be overcome. Specifically, a condition under which the existing machine-learning methods can be applied to complex dynamical systems

is the availability of large quantities of data for training. For physical systems accessible to continuous observation and measurements, this data requirement may not pose a significant challenge. However, for ecosystems, the available empirical datasets are often small and large datasets are generally notoriously difficult to obtain [31]. A compounding factor is that ecosystems are subject to constant disturbances [32], rendering noisy the available datasets. We note that, in recent years, machine learning has been applied to ecosystems [33] but not for predicting the long-term dynamical behavior or the attractor. For example, support vector machines and random forests were widely used in ecological science for tasks such as classifying invasive plant species, identifying the disease, forecasting the effects of anthropogenic [34, 35], estimating the hidden differential equations [36, 37], and reconstructing the “climate” of the entire system [38]. More recently, deep learning was applied in species recognition from video and audio analysis [39, 40].

To overcome the data-shortage difficulty, we exploit meta-learning [41, 42] to predict the long-term dynamics or the attractors of ecosystems. Meta-learning is a learning-to-learn paradigm that enhances the learning algorithm through experience accumulation across multiple episodes. Differing from the conventional machine learning approaches, a well-trained meta-learning framework can adapt to new tasks more swiftly and efficiently by leveraging its prior experience, thus reducing the necessity for extensive retraining and data collection. Owing to its unique features, meta-learning has found broad applications in fields such as computer vision [43], time series forecasting [44, 45], reinforcement learning [46], and identification of special quantum states [47]. Our goal

* Ying-Cheng.Lai@asu.edu

is to use meta-learning to reconstruct the “climate” of the target ecosystems, addressing the challenge of data scarcity. Specifically, we take advantage of a number of classical chaotic systems for training a conventional machine-learning architecture to gain “experience” with complex dynamics anticipated to occur in ecosystems, and then update or fine-tune the machine-learning algorithm using the small amount of available data from the actual ecosystem. The outcome is a well-adapted machine-learning framework capable of predicting the complex dynamical behavior of ecosystems with only limited data.

What machine learning architecture is appropriate to combine the meta-learning algorithm for predictive modeling of ecosystems? Recurrent neural networks [26, 48, 49] such as reservoir computing can be a candidate since the prediction requires historical information. For computational efficiency, we choose time-delayed feedforward neural networks (FNNs, see Appendix A) [21, 22, 27, 50], a variant of reservoir computing, where the present and historical information of the time series is input into the neural network through time-delayed embedding. With time-delayed FNNs, the meta-learning framework becomes adept at handling the intricate and often nonlinear temporal dependencies typical of ecological data, thereby enabling it to adapt and learn rapidly from new, limited, and noisy data.

In Sec. II, we describe our meta-learning scheme in detail. In Sec. III, successful prediction is demonstrated using three prototypical models: the chaotic Hastings-Powell system, a chaotic food chain, and the chaotic Lotka-Volterra system. Conclusions and discussion are offered in Sec. IV.

II. PROPOSED META-LEARNING FRAMEWORK

The proposed meta-learning framework consists of two distinct phases: adaptation and deployment. In the adaptation phase, a meta-learning neural-network architecture is exposed to a diverse array of synthetic datasets from a number of chaotic systems, allowing it to acquire a broad range of “experiences,” as illustrated in Fig. 1(a). This phase is crucial as it equips the neural networks with a versatile learning strategy, nurturing its ability to tackle new and unseen tasks from ecosystems. For meta-learning, the Reptile algorithm, a gradient-based method, is standard, as shown in Fig. 1(b). Figure 1(c) illustrates the deployment phase, in which the well-trained meta-learning scheme is applied to a specific ecosystem of interest. With only limited time series data from the target ecosystem, the scheme adeptly generates accurate long-term predictions of the “climate” of the system. An issue is, as compared with a vanilla machine-learning scheme (not meta-learning), how much data reduction can be achieved with our meta-learning approach. This issue can be addressed by performing nu-

merical experiments to determine the training duration required to achieve similar performance by meta-learning based framework and the conventional FNN model in reconstructing an ecosystem. Figure 1(d) presents a representative result from the Hastings-Powell ecosystem, where the meta-learning algorithm is able to reduce the length of the training data approximately five times.

The core of meta-learning is the gradient-based Reptile algorithm, as shown in Fig. 1(b). Articulated in 2018 [51], it has become a widely used method due to its simplicity and efficiency. In particular, differing from more complex meta-learning algorithms, Reptile requires less memory and computational resources, making it particularly suitable for ecosystem prediction from limited data. The algorithm begins by initializing the parameters. It then iteratively samples tasks, performs gradient descent, and updates the parameters. Let ϕ denote the parameter vector of the machine-learning architecture, s denote a task, and $\text{SGD}(L, \phi, k)$ be the function performing k gradient steps on loss L starting with ϕ and returning the final parameter vector. The Reptile algorithm can be described as:

- Initialize ϕ
- For iteration = 1, 2, ..., sample tasks s_1, s_2, \dots, s_n
- For $i = 1, 2, \dots, n$, compute $W_i = \text{SGD}(L_{s_i}, \phi, k)$
- Update $\phi \leftarrow \phi + \epsilon \frac{1}{k} \sum_{i=1}^n (W_i - \phi)$
- Continue

Consider the loss function $L_{s_i}(\phi)$. If ϕ_t are the parameters at step t , after k steps of gradient descent, the parameters are updated as:

$$W_i = \phi_t^k = \phi_t^{k-1} - \alpha \nabla_{\phi} L_{s_i}(\phi_t^{k-1}), \quad (1)$$

where α is the inner learning rate. This procedure is depicted in Fig 1(b1). Notably, if only one task is sampled, i.e., $s = 1$, then the algorithm will update the parameters vector toward the direction of the green arrow in Fig 1(b1). Afterward, the machine trains on different tasks, as shown in Fig 1(b2), where the initial parameter can be updated according to

$$\phi_{j+1} = \phi_j + \epsilon \frac{1}{k} \sum_{i=1}^n (W_i - \phi_j), \quad (2)$$

where ϵ is the outer learning rate. The outer loop procedure interpolates between the current initialization parameter vector ϕ and the task-specific parameter vector W_i , converging the parameters toward a solution close to the optimal solution manifold of each task s_i . It is worth emphasizing that the optimization goal of Reptile is not finding an optimal solution for a specific task but rather achieving a parameter vector ϕ that is close to the optimal solution manifold \mathcal{W}_s^* for each task s . This

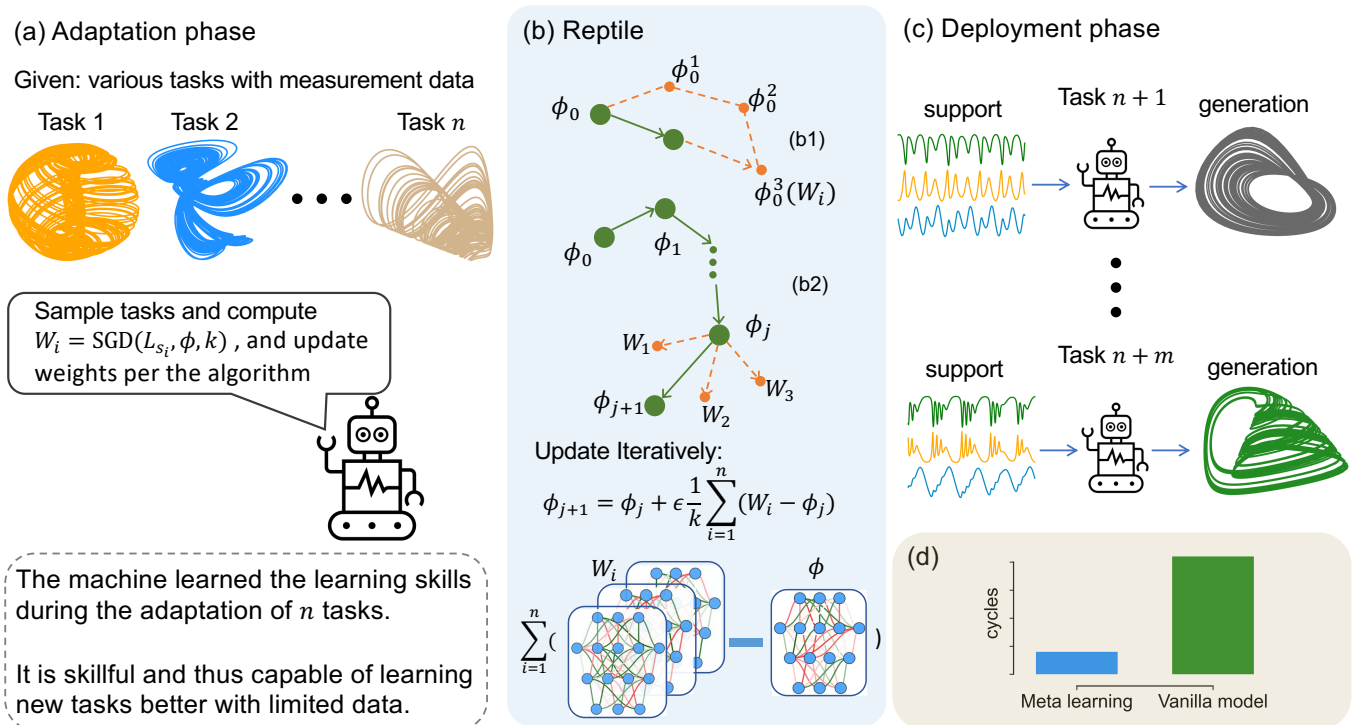


FIG. 1. Illustration of the proposed meta-learning framework for reconstructing ecosystems from limited data. (a) Adaptation phase, where the neural-network architecture is trained on various datasets from synthetic nonlinear chaotic systems so it learns the skill of learning and therefore can better learn the target ecosystem. (b) Illustration of the Reptile algorithm, a gradient-based meta-learning method - see text for details. (c) Deployment phase in which the trained meta-learning framework is applied to the target ecosystem, accomplishing the objective of predicting its long-term dynamics or attractor from limited time-series data. (d) An illustration of the comparison of the data requirements for achieving similar performance by our proposed meta-learning framework and standard machine-learning (vanilla model) in reconstructing the Hastings-Powell system.

can be formulated by minimizing the Euclidean distance between ϕ and \mathcal{W}_s^* :

$$\arg \min_{\phi} \mathbb{E}_s \left[\frac{1}{2} D(\phi, \mathcal{W}_s^*)^2 \right], \quad (3)$$

where $D(\phi, \mathcal{W}_s^*)$ denotes the distance. The gradient of this objective is given by

$$\begin{aligned} \nabla_{\phi} \mathbb{E}_s \left[\frac{1}{2} D(\phi, \mathcal{W}_s^*)^2 \right] &= \mathbb{E}_s \left[\frac{1}{2} \nabla_{\phi} D(\phi, \mathcal{W}_s^*)^2 \right] \\ &= \mathbb{E}_s [\phi - \mathcal{W}_s^*(\phi)]. \end{aligned} \quad (4)$$

where $\mathcal{W}_s^*(\phi)$ is the closest point in \mathcal{W}_s^* to ϕ . Each iteration of Reptile samples a task s and performs a stochastic gradient update:

$$\begin{aligned} \phi &= \phi - \epsilon \nabla_{\phi} \frac{1}{2} D(\phi, \mathcal{W}_s^*)^2 \\ &= \phi - \epsilon (\mathcal{W}_s^*(\phi) - \phi) \\ &= (1 - \epsilon) \phi + \epsilon \mathcal{W}_s^*(\phi). \end{aligned} \quad (5)$$

The method ensures that the updated parameters ϕ are not overly specific to any single task, but rather effective across a range of tasks. A comparative analysis of Reptile with other meta-learning methods such as MAML

(Model Agnostic Meta-Learning) is presented in Appendix B, and the differences between meta-learning and traditional transfer learning is discussed in Appendix C.

III. RESULTS

We present forecasting results for three ecosystems: the three-dimensional chaotic Hastings-Powell system [52], a three-species food chain system [53], and the Lotka-Volterra system [54] with three species. The hypothesis is that the observational data from each system is quite limited (to be quantified below), so it is necessary to invoke meta-learning by first training the neural network using synthetic time series from the computational models of a number of prototypical chaotic systems. Since the target ecosystems are three-dimensional, the chosen chaotic systems should have the same dimension. We use 27 such chaotic systems, as described in Appendix D. More specifically, during the adaptation phase, the neural-network architecture is trained and the values of the hyperparameters are determined with time-series data from the 27 synthetic systems. In the deployment phase, further training with appropriate adjustments to the hyperparameter values is done with the

limited data from the target ecosystem, followed by prediction of its long-term dynamics. It is worth noting that the continuous adjustments and fine-tuning of the parameters is the key feature that distinguishes meta-learning from transfer learning, as further explained in Appendix C. To demonstrate the superiority of meta-learning to conventional machine learning, we train the *same* neural-network architecture but using time series from the ecosystems only without any pre-training - the so-called vanilla or benchmark machine-learning scheme. For the vanilla scheme, typically much larger datasets are required to achieve comparable prediction performance by meta-learning.

Unless otherwise stated, the following computational settings are used. Given a target system, time series are generated numerically by integrating the synthetic system models with the time step $dt = 0.01$. The initial states of both the dynamical process and the neural network are randomly chosen from a uniform distribution. An initial segment of the time series is removed to ensure that the trajectory has reached the attractor. The training and testing data are obtained by sampling the time series at the interval Δ_s . Specifically, for the chaotic Hastings-Powell, food-chain, and Lotka-Volterra systems, we set $\Delta_s = 60dt = 0.6, 0.5,$ and 0.2 , corresponding to approximately $1/77, 1/83,$ and $1/71$ cycles of oscillation, respectively. The time series data are preprocessed by using min-max normalization so that they lie in the unit interval $[0,1]$. Considering the omnipresence of noise, we add Gaussian noise of amplitude $\sigma = 0.003$ to the normalized data. The training and predicting lengths of systems are set as 20,000 and 50,000, respectively. For the time-delayed FNN, the embedding dimension is 1,000, so the dimension of the input vector is 3,000 (three-dimensional systems). The neural network comprises three hidden layers with the respective sizes $[1024,512,128]$, and its output layer has the size of three (for three-dimensional target systems). The batch size is set to be 128. In meta-learning, we specify 20 inner iterations (I_i) and 30 outer iterations (I_o), with the inner and outer learning rates of $\alpha = 10^{-3}$ and $\epsilon = 1$, respectively. We apply Bayesian optimization to systematically determine the optimal hyperparameters and test the effects of the hyperparameters on the performance. Simulations are run using Python on two desktop computers with 32 CPU cores, 128 GB memory, and one RTX 4000 NVIDIA GPU.

To make the presentation succinct, in the main text we focus on the results from the chaotic Hastings-Powell system with a brief mentioning of the summarizing results for the three-species food chain and the chaotic Lotka-Volterra systems. The detailed results from the latter two systems are presented in Appendix E. It is worth noting that the chaotic Hastings-Powell system is a seminal model in population dynamics. It describes the feeding relationships in a food chain from prey to predators [52] and has inspired numerous variations and studies. The three-species food chain system [53] is in fact one variant

of the Hastings-Powell system, exhibiting a wide range of behaviors due to the incorporation of additional factors and bioenergetically derived parameters. There were also substantial works based on the original chaotic Hastings-Powell model [55–58], making it a benchmark and prototypical model in theoretical ecology.

A. Forecasting the chaotic Hastings-Powell system

The chaotic Hastings-Powell system [52] has three dynamical variables, corresponding to the resource, consumer, and predator abundances, respectively. The system is described by the following set of differential equations [59]:

$$\begin{aligned} \frac{dV}{dt} &= V(1 - V) - \frac{a_1 V H}{b_1 V + 1}, \\ \frac{dH}{dt} &= \frac{a_1 V H}{b_1 V + 1} - \frac{a_2 H P}{b_2 H + 1} - d_1 H, \\ \frac{dP}{dt} &= \frac{a_2 H P}{b_2 H + 1} - d_2 P, \end{aligned} \quad (6)$$

where V , H , and P are the biomass of the vegetation (or resource), herbivore (or consumer), and predator species, respectively. Alternatively, they can also represent vegetation, host, and parasitoid. The parameters a_1 , a_2 , b_1 , b_2 , d_1 , and d_2 are chosen to be biologically reasonable [52] as 5, 0.1, 3, 2, 0.4 and 0.01, respectively, which contain the information about the growth rate, the carrying capacity of the vegetation, etc.

To characterize the performance of long-term prediction of the attractor, we use two measures: deviation value (DV) and prediction stability, where the former describes the distance between the ground truth and predicted attractors and the latter (denoted as $R_s(DV_c)$) is the probability that meta-learning generates stable dynamical evolution of the target ecosystem in a fixed time window. The definition of the three-dimensional DV here is extended from its two-dimensional version [24]. To calculate the DV value, we place a uniform lattice in the three-dimensional phase space with the cell size $\Delta = 0.04$ and count the number of trajectory points in each cell for both the true and predicted attractors in a fixed time interval. The DV is given by

$$DV \equiv \sum_{i=1}^{m_x} \sum_{j=1}^{m_y} \sum_{k=1}^{m_z} \sqrt{(f_{i,j,k} - \hat{f}_{i,j,k})^2}, \quad (7)$$

where m_x , m_y , and m_z are the total numbers of cells in the x , y , and z directions, respectively, $f_{i,j,k}$ and $\hat{f}_{i,j,k}$ are the frequencies of visit to the cell (i, j, k) by the true and predicted trajectories, respectively. When the predicted trajectory leaves the square, we count them as if they belonged to the cells at the boundary where the true trajectory never visits. To obtain the prediction stability, we perform the experiment n times and calculate

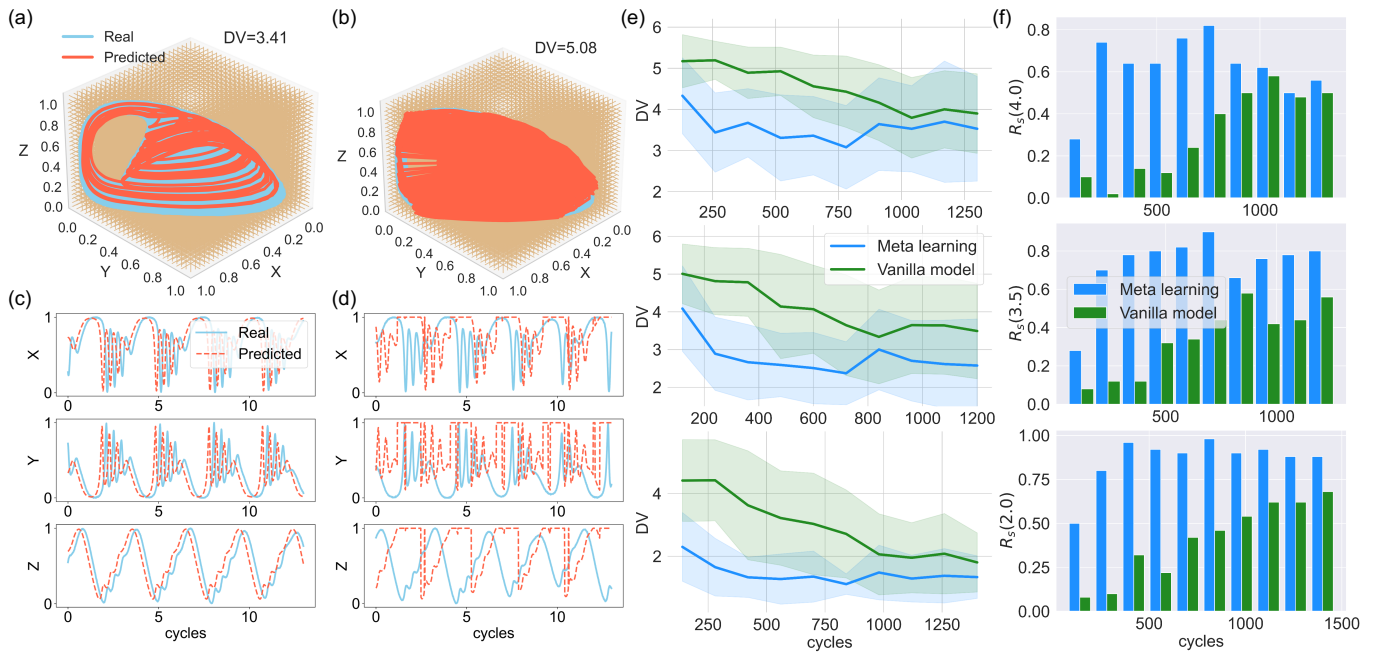


FIG. 2. Main result: long-term ecosystem prediction by the meta-learning and vanilla frameworks. (a,b) Attractor reconstruction by the two frameworks. (c,d) Intercepted snippets of the three time series of the ground truth and prediction by the two frameworks. (e) DV versus the training length for the meta-learning and vanilla frameworks. (f) Stability indicator of prediction ($R_s(DV_c)$) versus the training length for the meta-learning and vanilla frameworks. The upper, middle, and lower panels in (e) and (f) are from the chaotic Hastings-Powell, food chain, and Lotka-Volterra systems, respectively. To reduce the statistical fluctuations, the DVs, their shaded variabilities and the $R_s(DV_c)$ values are calculated from an ensemble of 50 independently trained neural machines.

the probability that the DV is below a predefined stable threshold, which is given by

$$R_s(DV_c) = \frac{1}{n} \sum_{i=1}^n [\text{DV} < \text{DV}_c], \quad (8)$$

where DV_c is the DV threshold, n is the number of iterations and $[\cdot] = 1$ if the statement inside is true and zero otherwise.

Figure 2 presents the comparative forecasting results, where Figs. 2(a) and 2(b) show the ground truth and the predicted attractors in the three-dimensional space by the meta-learning and vanilla frameworks, respectively. It can be seen that the attractor predicted by meta-learning has a lower DV, indicating that the predicted attractor is closer to the ground truth. Figures 2(c) and 2(d) display some representative time-series segments of the predicted and true attractors from the meta-learning and vanilla frameworks, respectively, using the same training data from the ecosystem. Apparently, the vanilla framework fails to predict the attractor correctly. Figures 2(e) and 2(f) show, respectively, the DV and prediction stability values versus the length of the training data from the three ecosystems. The meta-learning framework consistently yields a lower testing DV and higher prediction stability compared to those from the vanilla framework, indicating that meta-learning not only predicts more accurately the long-term dynamics on

the attractor but the results are also more stable and reliable. These advantages are particularly pronounced with shorter training lengths. In terms of the DV indicator, the vanilla framework requires approximately 5 to 7 times the amount of training data in meta-learning to achieve a similar level of performance. In terms of the prediction stability, the vanilla framework fails to match the performance of meta-learning, regardless of the training length.

In meta-learning, determining the optimal values of the hyperparameters is key to achieving reliable and accurate prediction results, which is done through standard Bayesian optimization. The procedure and the role of the optimal hyperparameter values are discussed in Appendix F.

B. Robustness against noise

It is useful to study how ecosystem forecasting is degraded by environmental noise for the meta-learning and vanilla frameworks. We consider normally distributed stochastic processes of zero mean and standard deviation σ to simulate the noise, which perturbs the time series point x to $x + \xi$ after normalization. Figure 3 illustrates the effects of the noise on predicting the three ecosystems via the meta-learning and vanilla frameworks, where 50 independent realizations are used to calculate the average

DV and the associated uncertainty. The results indicate that, for small noise (e.g., amplitude less than 10^{-2}), robust prediction performance as characterized by relatively low DVs can be achieved by meta-learning. In contrast, the DVs from the vanilla framework are higher. The results in Fig. 3 suggest that meta-learning is capable of yielding more accurate and robust prediction results.

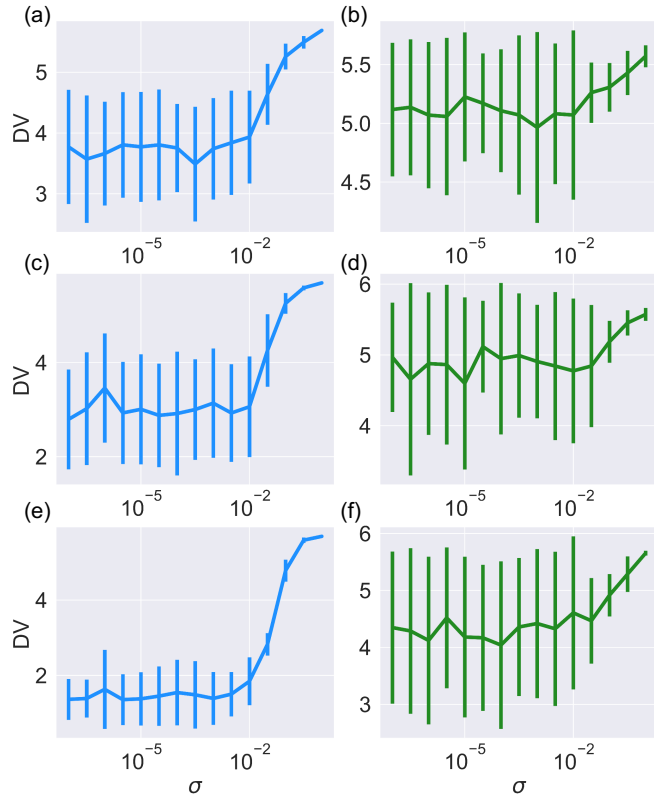


FIG. 3. Robustness of ecosystem forecasting against environmental noise. The top, middle, and bottom rows are attractor-prediction results for the chaotic Hastings-Powell, food chain, and Lotka-Volterra systems, respectively. The left and right columns are results from the meta-learning and vanilla frameworks, respectively. The same training lengths are used in all cases. The average prediction DV and the error bar are obtained from 50 independent training and testing runs. For meta-learning, the DVs remain small and approximately constant when the noise amplitude is below 10^{-2} . Overall, the prediction results from meta-learning are more accurate and robust against noise than the vanilla framework.

C. Optimal selection of synthetic systems for meta-learning

As described in Sec. II, the superiority of the meta-learning framework lies in gathering experience during the adaptation phase. However, indiscriminately utilizing different alternative chaotic systems as adaptation tasks in general does not lead to desired performances, and even worse, can destroy the training performance ow-

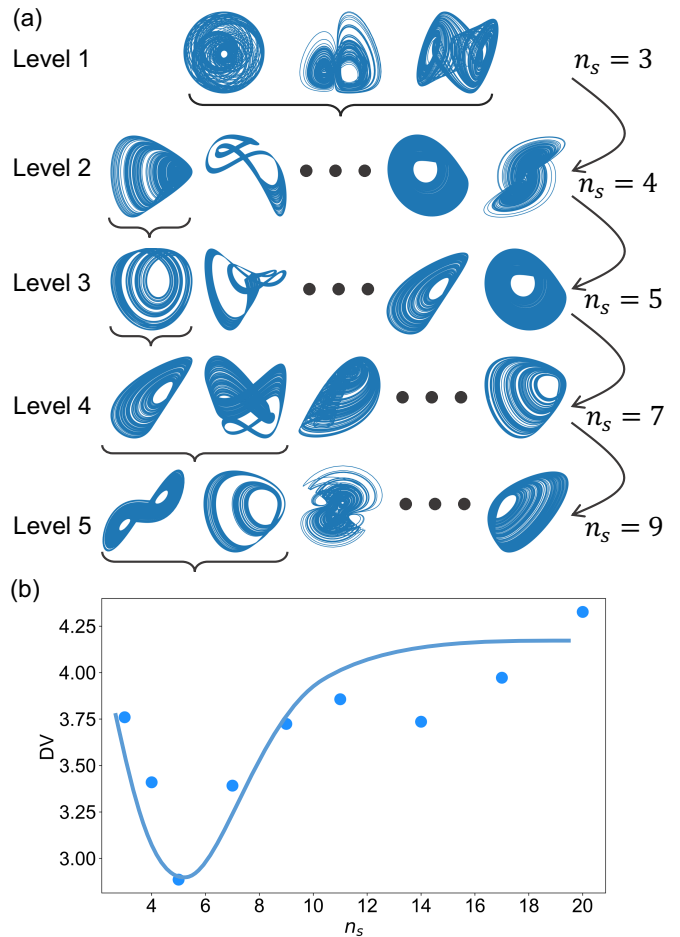


FIG. 4. Selecting the synthetic chaotic systems for the adaptation phase of meta-learning. (a) Illustration of greedy algorithm. Stated with the three systems in the sampled systems pool, one or several systems is (are) selected which lead to the best improvement in performance. (b) Ensemble averaged DV (with 50 independent realizations) versus the number of sampled systems pool n_s . As n_s increases, the average DV decreases rapidly but later increases again.

ing to the diversity of such systems. This raises the question of how to choose the proper adaptation systems for meta learning. To address this question, we employ the greedy algorithm to choose the optimal synthetic chaotic systems and use the chaotic Hastings-Powell system as a testing case for this algorithm. The test is performed, as follows. At each iteration, we perform a testing loop that involves adding a candidate system to the existing pool of chosen systems and monitoring the corresponding decrease in the resulting DV. Afterward, we remove this system and test another candidate system. After looping over all the candidate systems, we select one or several systems that lead to the maximal reduction of the average DV value calculated from 50 independent runs. Once a system has been selected, it will become a member of the chosen system pool in the iterative process that follows.

Figure 4(a) depicts this selection process, where the

initial sampled system pool is $n_s = 3$. Looping at level one informs us that a new system should be added to the sampled system pool, so at Level two the pool size becomes $n_s = 4$. Repeating this process iteratively, we collect the ensemble-averaged DV and the corresponding sampled system pool n_s , as shown in Fig. 4(b). We observe that the average DV decreases rapidly as the number of systems increases from one to twenty but begins to increase again when more systems are included. Consequently, guided by the greedy algorithm, we select the five most effective systems: Aizawa, Bouali, Chua, Sprott third, and Sprott fourteen (See Appendix D for a detailed description of these systems). It is worth noting that we do not expect the greedy algorithm to produce globally optimal solutions in the space of all possible chaotic systems. It might miss useful systems, each alone would not reduce the DV but their combination would. Considering that this feature selection process is NP-hard, finding some locally optimal solutions is reasonable. This also implies that, while the performance of meta-learning is remarkable, there is ample room for improvement.

IV. DISCUSSION

Exploiting machine learning to predict the behaviors of dynamical systems has attracted extensive research in recent years, and it has been demonstrated that modern machine learning can solve challenging problems in complex and nonlinear dynamics that were previously deemed unsolvable. However, machine-learning algorithms often require extensive data for training, and this presents a significant challenge for ecosystems. Indeed, the observational datasets for ecosystems, especially those described by the population dynamics, are often small, preventing a straightforward and direct application of machine learning to these systems.

This work develops an “indirect,” meta-learning framework for forecasting the long-term dynamical behaviors of chaotic ecosystems through a faithful reconstruction of the attractor using only limited data. Given a chaotic ecosystem of interest, the idea is to use a large number of alternative chaotic systems of the same dimension, which can be simulated to generate massive training data for a suitable machine-learning scheme such as the time-delayed feedforward neural-network architecture. The neural networks are trained using the synthetic data first, and are then “fine-tuned” with the data from the actual target ecosystem. As a result of the pre-training or first-stage training for adaptation, the neural machine is sufficiently exposed to the climate of the dynamical evolution of characteristically similar systems, which can then be readily adapted to the ecosystem. Specifically, we employed Reptile as the meta-learning algorithm. During the adaptation phase, the algorithm begins by gaining “experience” from learning a synthetic chaotic system. This process continues with data from different non-ecological chaotic systems until the machine is well-

trained, experienced, and able to learn new tasks with limited data. In the deployment phase, the neural machine is further trained using the limited data from the target ecosystem - the second-stage training. We emphasize that the first-stage training uses massive data from a large number of model chaotic systems, and the second-stage training is done with limited data from the target ecosystem. After the second-stage training, the neural machine is capable of generating the correct attractor of the ecosystem, realizing accurate and reliable forecasting of its long-term dynamics. It is worth noting that, while the systems used in the adaptation phase of the training have characteristically similar attractors, their detailed dynamical evolution can still be quite distinct. It can then be intuitively anticipated that the meta-learning framework will not have any advantage over the vanilla model with respect to short-term prediction of the state evolution (see Appendix G).

One feature of our meta-learning framework is the integration of time-delayed feedforward neural networks for processing sequential data. It incorporates the concept of time delays into the conventional FNN architecture so as to take the advantage of the present and historical information in the time series. We have tested the meta-learning framework on three benchmark ecosystems. In all cases, more accurate and robust prediction was achieved by the meta-learning based framework, whereas the vanilla model requires 5 – 7 times the training data to achieve a similar performance. Issues such as the effect of noise and the number of synthetic systems used in the adaptation phase of the training were addressed.

In general, meta-learning is a powerful machine-learning tool for solving prediction and classification problems in situations where the available data amount is small. A recent example is detecting quantum scars in systems with chaotic classical dynamics. In particular, in a closed quantum system in the semiclassical regime where the particle wavelength is much smaller than the system size, a vastly large number of eigenstates are permitted, among which are those whose wavefunctions are not uniformly distributed in the physical space but instead concentrate on some classical periodic orbits of low periods. The emergence of such scarring eigenstates is counterintuitive, as the classical trajectories are uniform due to ergodicity [60, 61]. In the field of quantum chaos, traditionally identifying quantum scarring states was done in a “manual” way through a visual check of a large number (e.g., 10^4) of eigenstates [62]. This was challenging as the percentage of scarring states is typically small - less than 10% of all the eigenstates. A recent work demonstrated that meta-learning can be powerful for accurately detecting quantum scars in a fully automated and efficient way [47], where a standard large dataset called Omniglot from the field of image classification was used for training in the adaptation phase.

Our meta-learning framework incorporating time-delayed FNNs possesses a high level of sensitivity to the

temporal variations in the data, making it potentially feasible for extension beyond ecosystems to challenging problems such as epidemic spread prediction and traffic forecasting, where effective data collection is often a hurdle. There is also room for enhancing the performance of the framework. For example, in the present work, we employed the greedy algorithm for selecting synthetic chaotic systems for the adaptation phase of the training and implement meta-learning using the Reptile algorithm. Alternative algorithms can be exploited to achieve better performance.

DATA AND CODE AVAILABILITY

Data and code are available upon request and will be available on GitHub.

ACKNOWLEDGMENT

This work was supported by the Air Force Office of Scientific Research under Grant No. FA9550-21-1-0438 and by the Army Research Office.

Appendix A: Time-delayed Feedforward neural networks

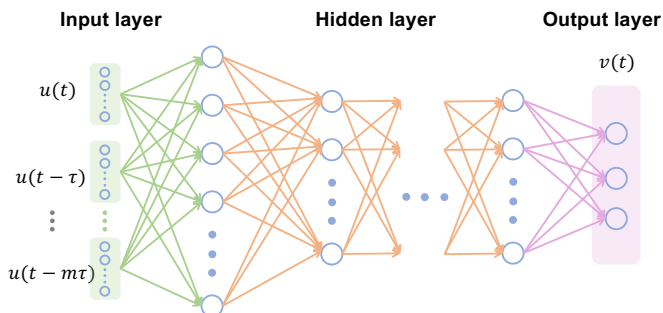


FIG. 5. Architecture of a time-delayed feedforward neural network. There are three main components: the input layer, a number of hidden layers, and the output layer, where $u(t), u(t - \tau), \dots, u(t - m\tau)$ are the present and historical signal with τ being the time delay and m being the embedding dimension. The output is $v(t)$.

FNNs have a straightforward neural-network architecture. Compared with recurrent neural networks, information in an FNN moves in only one direction, i.e., the neurons only process the information forward through the chain of connections from the input to the output. An FNN consists of layers of neurons, where each neuron in each layer has direct connections to the neurons in the subsequent layer. These connections are characterized by weights to be adjusted during the training process. A sufficiently large FNN can be deemed as a universal

nonlinear approximator, which can capture the hidden complex relationship between the input and output data.

We use time-delayed FNNs [22, 27], as illustrated in Fig. 5, which incorporates time delays into the original FNN architecture so as to instill certain memory function into the original FNN. A time-delayed FNN provides the present and historical information of the time series, making it suitable for processing sequential data. Specifically, to embed the memory into a FNN, we use the present signal $u(t)$ and the historical signals $u(t - \tau), \dots, u(t - m\tau)$ as the inputs, where τ is the delayed time and m is the system dimension.

The loss function is the mean squared error (MSE), which quantifies the difference between the predicted output and the true output:

$$\text{MSE} = \frac{1}{N_m} \sum_{i=1}^{N_m} (\hat{y}_i - y_i)^2, \quad (\text{A1})$$

where N_m is the number of samples, \hat{y} and y are the predicted and true outputs, respectively. We utilize the ReLU (Rectified Linear Unit) activation function defined as $f(x) = \max(0, x)$. It introduces nonlinearity into the network, enabling it to learn complex patterns and relationships in the data, and it is computationally efficient. In addition, for optimizing the weights in a time-delayed FNN, we employ the stochastic gradient descent (SGD) algorithm, specifically the Adam (Adaptive Moment Estimation) variant, which computes the adaptive learning rates for each parameter by storing exponentially decaying average of the past squared gradients. The adaptive ability makes it suitable and effective for handling non-convex optimization problems commonly arisen in neural networks.

Appendix B: Reptile algorithm

Here we provide a mathematical description of the Reptile algorithm [51]. We compare it with MAML [41] and FOMAML (First Order MAML), focusing on the case of two gradient steps ($k = 2$) in the SGD process. Similar to the definitions in the main text, we denote L^0 and L^1 as the losses for different batches of data. Let ϕ be the parameter vector and α be the step size. For simplicity, we annotate $g_j^i = \nabla_{\phi} L^i(\phi_j)$ and $h_j^i = \nabla_{\phi}^2 L^i(\phi_j)$. The parameter updates after two SGD steps are

$$\phi_0 = \phi \quad (\text{B1})$$

$$\phi_1 = \phi_0 - \alpha \nabla_{\phi} L^0(\phi_0) = \phi_0 - \alpha g_0^0 \quad (\text{B2})$$

$$\phi_2 = \phi_1 - \alpha \nabla_{\phi} L^1(\phi_1) = \phi_0 - \alpha g_0^0 - \alpha g_1^1 \quad (\text{B3})$$

The gradient of Reptile, MAML, and FOMAML are defined as:

$$g_{\text{Reptile}} = (\phi_0 - \phi_2)/\alpha = g_0^0 + g_1^1, \quad (\text{B4})$$

$$\begin{aligned} g_{\text{MAML}} &= \nabla_{\phi_0} L^1(\phi_1) \\ &= \nabla_{\phi_1} L^1(\phi_1)(I - \alpha \nabla_{\phi_1}^2 L^0(\phi_0)) \\ &= g_1^1 - \alpha h_0^0 g_1^1, \end{aligned} \quad (\text{B5})$$

$$g_{\text{FOMAML}} = \nabla_{\phi_1} L^1(\phi_1) = g_1^1. \quad (\text{B6})$$

Applying Taylor expansion to g_1^1 at ϕ_0 , we get:

$$\begin{aligned} g_1^1 &= \nabla_{\phi_0} L^1(\phi_1) \\ &= \nabla_{\phi_0} L^1(\phi_0) + \nabla_{\phi_0}^2 L^1(\phi_0)(\phi_1 - \phi_0) + O(\alpha^2) \\ &= g_0^1 - \alpha h_0^0 g_0^1 + O(\alpha^2) \end{aligned} \quad (\text{B7})$$

Substituting this into the gradients of Reptile, MAML, and FOMAML in B4 to B6, we get

$$g_{\text{Reptile}} = g_0^0 + g_0^1 - \alpha h_0^0 g_0^1 + O(\alpha^2) \quad (\text{B8})$$

$$g_{\text{MAML}} = g_0^1 - \alpha h_0^0 g_0^1 - \alpha h_0^0 g_0^1 + O(\alpha^2) \quad (\text{B9})$$

$$g_{\text{FOMAML}} = g_0^1 - \alpha h_0^0 g_0^1 + O(\alpha^2) \quad (\text{B10})$$

During the training, we use batches 0 and 1 to calculate losses L^0 and L^1 , respectively. Let $\mathbb{E}_{s,0,1}$ be the expectation value over the two batches in the task s and let

$$\text{AvgGrad} = \mathbb{E}_{s,0,1}[g_0^0] = \mathbb{E}_{s,0,1}[g_0^1]$$

be the gradient of the expected loss. The negative direction of AvgGrad brings ϕ towards the minimum of the ‘‘joint training’’ problem so as to achieve better task performance. Let

$$\begin{aligned} \text{AvgGradInner} &= \mathbb{E}_{s,0,1}[h_0^1 g_0^0] = \frac{1}{2} \mathbb{E}_{s,0,1}[h_0^1 g_0^0 + h_0^0 g_0^1] \\ &= \frac{1}{2} \mathbb{E}_{s,0,1}[\nabla_{\phi}(g_0^0 g_0^1)]. \end{aligned}$$

The negative direction of AvgGradInner thus increases the inner product between gradients of different batches for the given task so as to yield better generalization.

The gradients for the meta-learning algorithms, aiming for optimal task performance and generalization, can be summarized as:

$$\mathbb{E}_{s,0,1}[g_{\text{Reptile}}] = 2\text{AvgGrad} - \alpha \cdot \text{AvgGradInner} + O(\alpha^2), \quad (\text{B11})$$

$$\mathbb{E}_{s,0,1}[g_{\text{MAML}}] = \text{AvgGrad} - 2\alpha \cdot \text{AvgGradInner} + O(\alpha^2), \quad (\text{B12})$$

$$\mathbb{E}_{s,0,1}[g_{\text{FOMAML}}] = \text{AvgGrad} - \alpha \cdot \text{AvgGradInner} + O(\alpha^2), \quad (\text{B13})$$

where each gradient expression first leads to the minimum of the expected loss over tasks, and then the higher order AvgGradInner term enables fast learning.

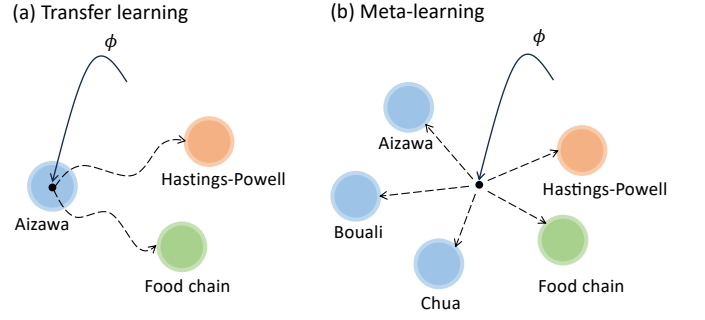


FIG. 6. Illustration of transfer learning versus meta-learning. The solid lines denote the learning of the initial parameters, and the dashed lines show the path of fine-tuning. Blue circles represent the adaptation tasks and other colored circles indicate the deployment tasks.

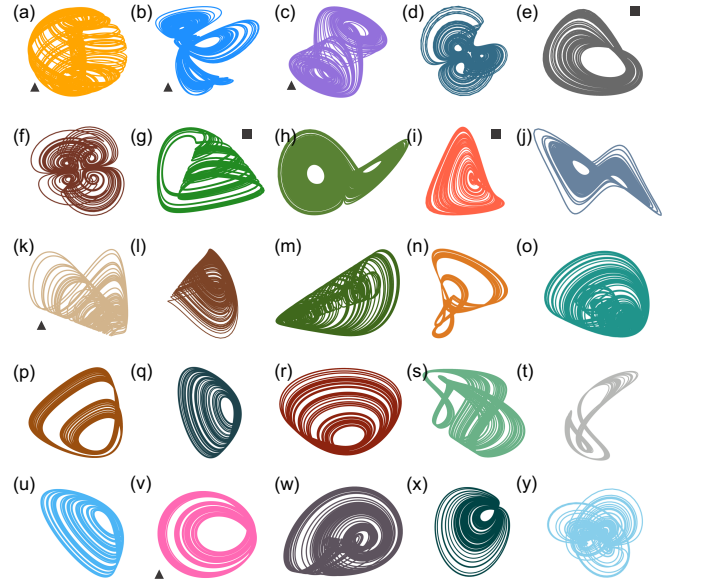


FIG. 7. Illustration of the synthetic chaotic systems for adaptation learning during the training and the target ecosystems. (a) Aizawa, (b) Bouali, (c) Chua, (d) Dadras, (e) Food chain, (f) Four wing, (g) Hastings-Powell, (h) Lorenz, (i) Lotka-Volterra, (j) Rikitake, (k-y) Sprott systems. The systems chosen by the greedy algorithm in the adaptation phase are marked by triangles and the target ecosystems are marked by rectangles.

Appendix C: Meta-learning versus transfer learning

It is worth discussing the difference between transfer learning and meta-learning. Transfer learning, often referred to as fine-tuning, is a technique where a neural network trained for one task is applied to another related task. It involves leveraging the pre-trained layers of the network, where some layers are ‘‘frozen’’ (i.e., their weights are not updated), while others are adjusted or added to tailor the network to the new task. This approach capitalizes on the existing knowledge of the network, particularly its ability to recognize and utilize data

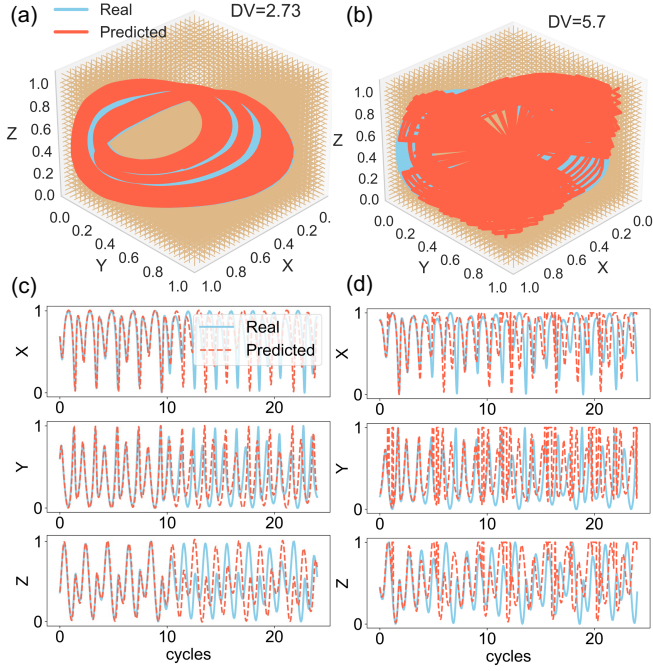


FIG. 8. Long-term prediction of the chaotic three-species food chain system by meta-learning and standard frameworks. (a,b) Reconstructed attractor by the two frameworks. (c,d) Intercepted snippets of the ground truth and machine-learning prediction. The results in the left and right columns are generated by the meta-learning and the standard frameworks, respectively.

patterns. It is especially effective when the tasks share common features or structures. Meta-learning, or “learning to learn,” is at a higher level. It focuses on understanding and optimizing the learning process itself rather than acquiring knowledge from the data directly. Meta-learning algorithms accumulate experiences from various learning tasks and develop strategies to efficiently optimize the parameters of a neural network. This process enables the network to quickly adapt to new tasks, learning not just specific data patterns but the underlying principles of learning and optimization.

In general, in meta-learning, knowledge is learned but not directly (e.g., through hyperparameters), where learning can be related to optimization [63]. In fact, meta-learning optimizes the hyperparameters of the networks that were not trained, whereas transfer learning takes a well-trained network and only adjusts some parts, given a new task. Empirically, transfer learning requires the trained and adapted tasks to be more similar. Figure 6 presents a comparison between transfer learning and meta-learning, where transfer learning trains a neural network specifically for the source task (Aizawa system), and fine-tunes the system to each target task (e.g., the Hastings-Powell and food-chain systems). In comparison, meta-learning trains the neural network to adapt and fine-tune both source tasks and target tasks, where

the learned knowledge is not directly reflected in the neural network parameters but is embedded in the parameter optimization procedure.

Appendix D: Details of the synthetic chaotic systems for adaptation and target ecosystems

The synthetic chaotic systems employed during the adaptation phase of the training and the target ecosystem are illustrated in Fig. 7. The system equations and parameters used to simulate the time series for these systems are listed in Tabs. I and II.

Appendix E: Results of long-term prediction for two ecosystems

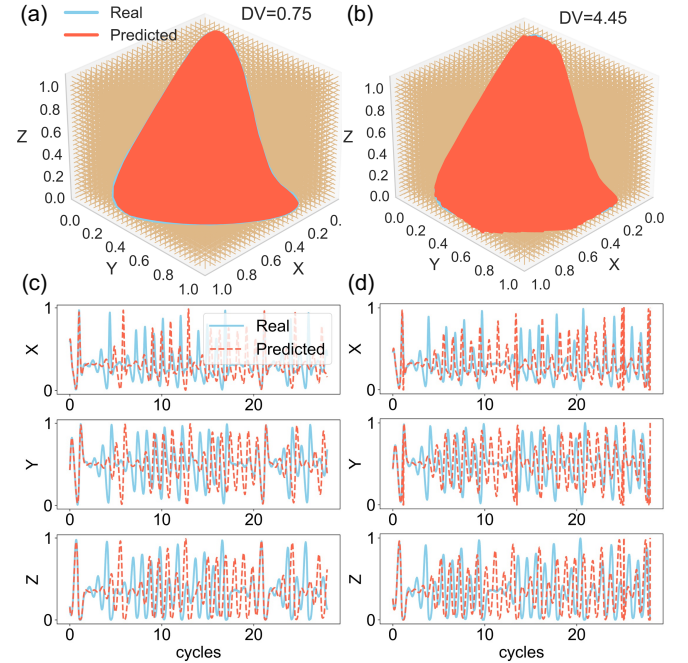


FIG. 9. Long-term prediction of the chaotic Lotka-Volterra system by meta-learning and standard frameworks. (a,b) Reconstructed attractor by the two frameworks. (c,d) Intercepted snippets of the ground truth and machine-learning prediction. The results in the left and right columns are generated by the meta-learning and the standard frameworks, respectively.

The three-species food chain system is described by the following set of nonlinear differential equations:

$$\begin{aligned}
 \frac{dR}{dt} &= R\left(1 - \frac{R}{K}\right) - \frac{x_c y_c C R}{R + R_0}, \\
 \frac{dC}{dt} &= x_c C \left(\frac{y_c R}{R + R_0} - 1\right) - \frac{x_p y_p P C}{C + C_0}, \\
 \frac{dP}{dt} &= x_p P \left(\frac{y_p C}{C + C_0} - 1\right),
 \end{aligned} \quad (E1)$$

TABLE I. Synthetic chaotic systems and target ecosystems

Systems	Equations	Parameters
Aizawa	$\begin{aligned}\dot{x} &= (z - b)x - dy \\ \dot{y} &= dx + (z - b)y \\ \dot{z} &= c + az - z^3/3 - (x^2 + y^2)(1 + e^z) + fzx^3\end{aligned}$	$a = 0.95, b = 0.7, c = 0.6$ $d = 3.5, e = 0.25, f = 0.1$
Bouali [64]	$\begin{aligned}\dot{x} &= x(a - y) + \alpha z \\ \dot{y} &= -y(b - x^2) \\ \dot{z} &= -x(c - sz) - \beta z\end{aligned}$	$\alpha = 0.3, \beta = 0.05$ $a = 4, b = 1, c = 1.5, s = 1$
Chua [65]	$\begin{aligned}\dot{x} &= \alpha(y - x - ht) \\ \dot{y} &= \gamma(x - y + z) \\ \dot{z} &= -\beta y\end{aligned}$	$\alpha = 15.6, \gamma = 1, \beta = 28$ $\mu_0 = -1.143, \mu_1 = -0.714$ $ht = \mu_1 x + 0.5(\mu_0 - \mu_1)(x + 1 - x - 1)$
Dadras [66]	$\begin{aligned}\dot{x} &= y - ax + byz \\ \dot{y} &= cy - xz + z \\ \dot{z} &= dxy - ez\end{aligned}$	$a = 3, b = 2.7$ $c = 1.7, d = 2, e = 9$
Four wing [67]	$\begin{aligned}\dot{x} &= ax + yz \\ \dot{y} &= bx + cy - xz \\ \dot{z} &= -z - xy\end{aligned}$	$a = 0.2, b = 0.01, c = -0.4$
Lorenz [68]	$\begin{aligned}\dot{x} &= \sigma(y - x) \\ \dot{y} &= x(\rho - z) - y \\ \dot{z} &= xy - \beta z\end{aligned}$	$\sigma = 10, \rho = 28, \beta = 2.67$
Rikitake [69]	$\begin{aligned}\dot{x} &= -\mu x + zy \\ \dot{y} &= -\mu y + x(z - a) \\ \dot{z} &= 1 - xy\end{aligned}$	$\mu = 2, a = 5$
Rossler [70]	$\begin{aligned}\dot{x} &= -(y + z) \\ \dot{y} &= x + ay \\ \dot{z} &= b + z(x - c)\end{aligned}$	$a = 0.2, b = 0.2, c = 5.7$
Food chain	$\begin{aligned}\dot{R} &= R(1 - R/K) - x_c y_c CR / (R + R_0) \\ \dot{C} &= x_c C (y_c R / (R + R_0) - 1) - x_p y_p PC / (C + C_0) \\ \dot{P} &= x_p P (y_p C / (C + C_0) - 1)\end{aligned}$	$K = 0.98, y_c = 2.009, y_p = 2.876$ $x_c = 0.4, x_p = 0.08$ $R_0 = 0.16129, C_0 = 0.5$
Hastings-Powell	$\begin{aligned}\dot{V} &= V(1 - V) - a_1 VH / (b_1 V + 1) \\ \dot{H} &= a_1 VH / (b_1 V + 1) - a_2 HP / (b_2 H + 1) - d_1 H \\ \dot{P} &= a_2 HP / (b_2 H + 1) - d_2 P\end{aligned}$	$a_1 = 5, a_2 = 0.1$ $b_1 = 3, b_2 = 2$ $d_1 = 0.4, d_2 = 0.01$
Lotka-Volterra	$\dot{P}_i = r_i P_i (1 - \sum_{j=1}^N a_{ij} P_j)$	$r_i = [1; 0.72; 1.53; 1.27]$ $a_{ij} = \begin{pmatrix} 1 & 1.09 & 1.52 & 0 \\ 0 & 1 & 0.44 & 1.36 \\ 2.33 & 0 & 1 & 0.47 \\ 1.21 & 0.51 & 0.35 & 1 \end{pmatrix}$

where R , C , and P are the population densities of the resource, consumer, and predator species, respectively. The constant parameters K , x_c , y_c , x_p , y_p , R_0 , C_0 are set to be 0.98, 0.4, 2.009, 0.08, 2.876, 0.16129, 0.5, respectively, as stipulated by a bioenergetics argument [53]. The statistical results have been shown in the second row of Figs. 2(e) and 2(f) in the main text, which compare the DV and prediction stability between the meta-learning and standard frameworks. Across all training

cycles, the meta-learning framework consistently demonstrates a lower testing DV and higher prediction stability than the standard model. Figure 8 exemplifies the results of reconstructing the attractor, where the left and right columns are generated by meta-learning and standard frameworks, respectively. It can be seen that meta-learning predicted attractor possesses a more similar ‘‘climate’’ to the ground truth.

TABLE II. Chaotic sprout systems [71]

Case	Equations
0	$\dot{x} = y, \dot{y} = -x + yz, \dot{z} = 1 - y^2$
1	$\dot{x} = yz, \dot{y} = x - y, \dot{z} = 1 - xy$
2	$\dot{x} = yz, \dot{y} = x - y, \dot{z} = 1 - x^2$
3	$\dot{x} = -y, \dot{y} = x + z, \dot{z} = xz + 3y^2$
4	$\dot{x} = yz, \dot{y} = x^2 - y, \dot{z} = 1 - 4x$
5	$\dot{x} = y + z, \dot{y} = -x + 0.5y, \dot{z} = x^2 - z$
6	$\dot{x} = 0.4x + z, \dot{z} = xz - y, \dot{y} = -x + y$
7	$\dot{x} = -y + z^2, \dot{y} = x + 0.5y, \dot{z} = xz$
8	$\dot{x} = -0.2y, \dot{y} = x + z, \dot{z} = x + y^2 - z$
9	$\dot{x} = 2z, \dot{y} = -2y + z, \dot{z} = -x + y + y^2$
10	$\dot{x} = xy - z, \dot{y} = x - y, \dot{z} = x + 0.3z$
11	$\dot{x} = y + 3.9z, \dot{y} = 0.9x^2 - y, \dot{z} = 1 - x$
12	$\dot{x} = -z, \dot{y} = -x^2 - y, \dot{z} = 1.7 + 1.7x + y$
13	$\dot{x} = -2y, \dot{y} = x + z^2, \dot{z} = 1 + y - 2z$
14	$\dot{x} = y, \dot{y} = x - z, \dot{z} = x + xz + 2.7y$
15	$\dot{x} = 2.7y + z, \dot{y} = -x + y^2, \dot{z} = x + y$
16	$\dot{x} = -z, \dot{y} = x - y, \dot{z} = 3.1x + y^2 + 0.5z$
17	$\dot{x} = 0.9 - y, \dot{y} = 0.4 + z, \dot{z} = xy - z$
18	$\dot{x} = -x - 4y, \dot{y} = x + z^2, \dot{z} = 1 + x$

The Lotka-Volterra system is described by

$$\frac{dP_i}{dt} = r_i P_i \left(1 - \sum_{j=1}^N a_{ij} P_j\right), \quad (\text{E2})$$

where r_i is the growth rate of species i and a_{ij} describes the extent to which species j competes with i for resources. We use the four-species competitive Lotka-Volterra model defined by [54], where the parameters are set as

$$r_i = \begin{bmatrix} 1 \\ 0.72 \\ 1.53 \\ 1.27 \end{bmatrix}, \quad a_{ij} = \begin{bmatrix} 1 & 1.09 & 1.52 & 0 \\ 0 & 1 & 0.44 & 1.36 \\ 2.33 & 0 & 1 & 0.47 \\ 1.21 & 0.51 & 0.35 & 1 \end{bmatrix}, \quad (\text{E3})$$

The comparative statistical results have been shown in the last row of Figs. 2(e) and 2(f) in the main text.

Similar to the results from the chaotic food-chain system, the meta-learning framework consistently demonstrates a lower testing DV, and higher prediction stability than the standard framework. Figure 9 shows an example of attractor reconstruction, where the left and right columns are generated by meta-learning and standard frameworks, respectively. Meta-learning generates an attractor that has a more similar “climate” to the ground truth.

Appendix F: Hyperparameter optimization

TABLE III. Optimal hyperparameter values

Hyperparameters	Descriptions
$I_o=30$	Number of meta-learning outer iterations
$I_i=20$	Number of meta-learning inner iterations
$\epsilon=1.0$	Meta-learning learning rate
$\alpha=1 \times 10^{-3}$	Neural network base learning rate
$\beta=0.9$	Gradient descent momentum term
$n_t=2$	Task sampling number

In our meta-learning based time-delayed FNN framework, the optimal hyperparameter values are determined through Bayesian optimization, which are listed in Table III. To appreciate The role of the optimal hyperparameters, we examine the effects of varying the hyperparameters on the prediction performance.

Figure 10 shows the influence of the task sampling number n_t that determines the number of tasks selected in each meta-learning iteration. Considering the tradeoff between high performance and computational efficiency, we select $n_t = 2$. Figure 11 demonstrates the effect I_o and I_i , the numbers of meta-learning outer and inner iterations, respectively, on the performance of predicting the long-term dynamics of the ecosystems, where the color-coded values of the $R_s(DV_c)$ are displayed in the two-dimensional parameter plane (I_o, I_i) . Specifically, I_o is the number of times of meta-learning updates in the adaptation phase and I_i is the epoch of the neural network to learn each task. As I_o and I_i increase, the performance is dramatically improved. For high performance and low computational time, we select $I_o = 30$ and $I_i = 20$.

Figure 12 demonstrates the effect of meta-learning learning rate ϵ and neural network base learning rate α on the performance of predicting the attractors of the ecosystems, where the color-coded values of the $R_s(DV_c)$ are displayed in the two-dimensional parameter plane (ϵ, α) . Particularly, the learning rate controls the step size of each outer iteration taken, and the neural network base learning rate controls the learning step size of the inner iterations. It can be seen that the prediction performance depends more on α than on ϵ . we select $\epsilon = 1.0$ and $\alpha = 1 \times 10^{-3}$ in our work.

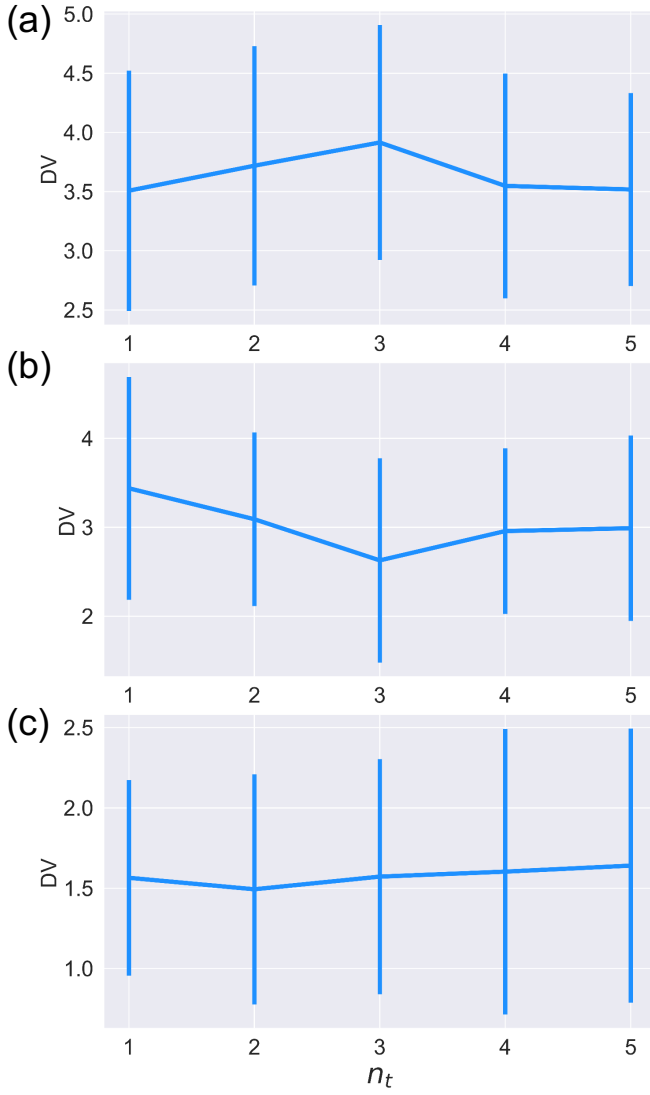


FIG. 10. Effect of task sampling number n_t on long-term prediction performance. (a-c) DV versus n_t for the Hastings-Powell, food-chain, and Lotka-Volterra systems, respectively. Each data point and the associated error bar are obtained from 50 independent runs.

Appendix G: Short-term prediction

While the primary focus of our study is on reducing the training time for long-term prediction, we have also studied the short-term prediction for both the meta-learning and standard frameworks. Here, by “short-term” we mean a few cycles of oscillations of the target ecosystem. To be concrete, for the Hastings-Powell, food-chain, and Lotka-Volterra systems, we use 300, 400, and 360 time steps, corresponding approximately to 3.9, 4.8, and 5.1 cycles of oscillation, respectively. To characterize the performance of short-term prediction, we use the root-

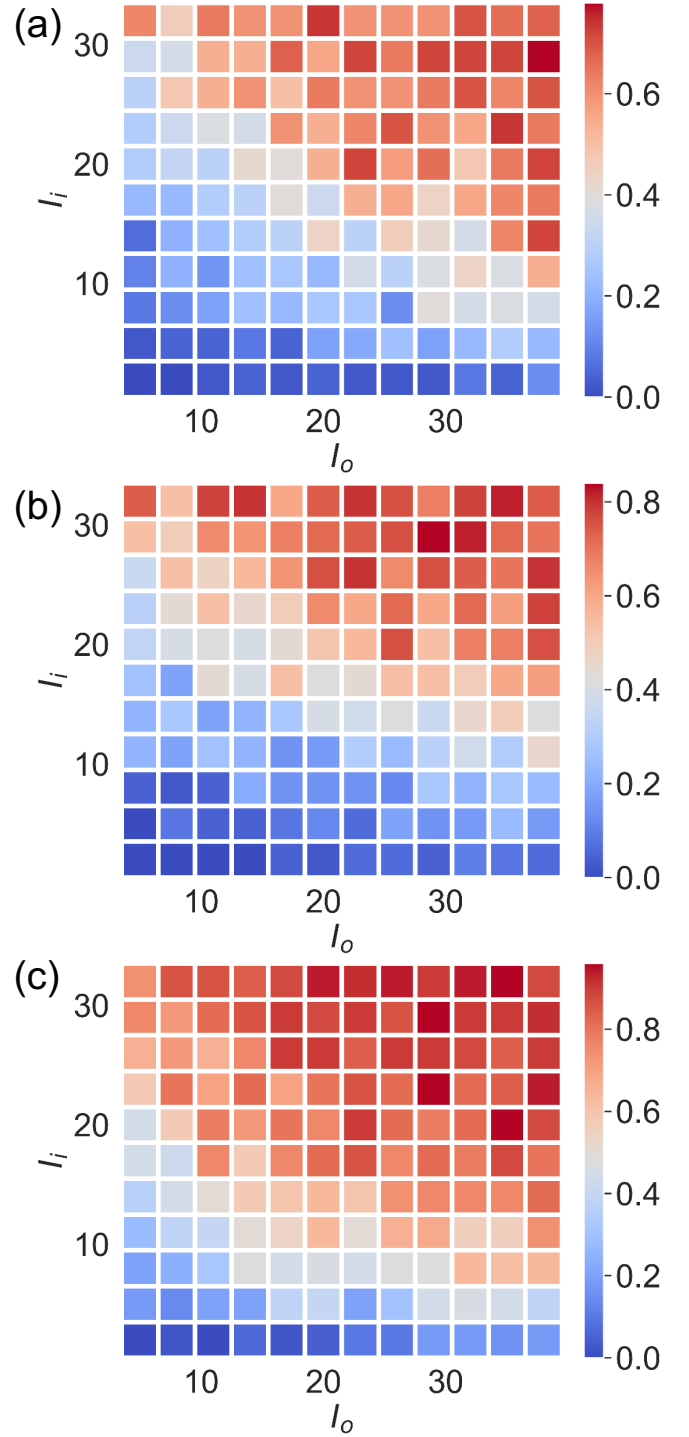


FIG. 11. Effects of hyperparameters I_o and I_i on the prediction performance. (a-c) Color-coded DV values in the plane of the two hyperparameters for the Hastings-Powell, food-chain, and Lotka-Volterra systems, respectively. Each DV value is obtained using 50 statistical realizations.

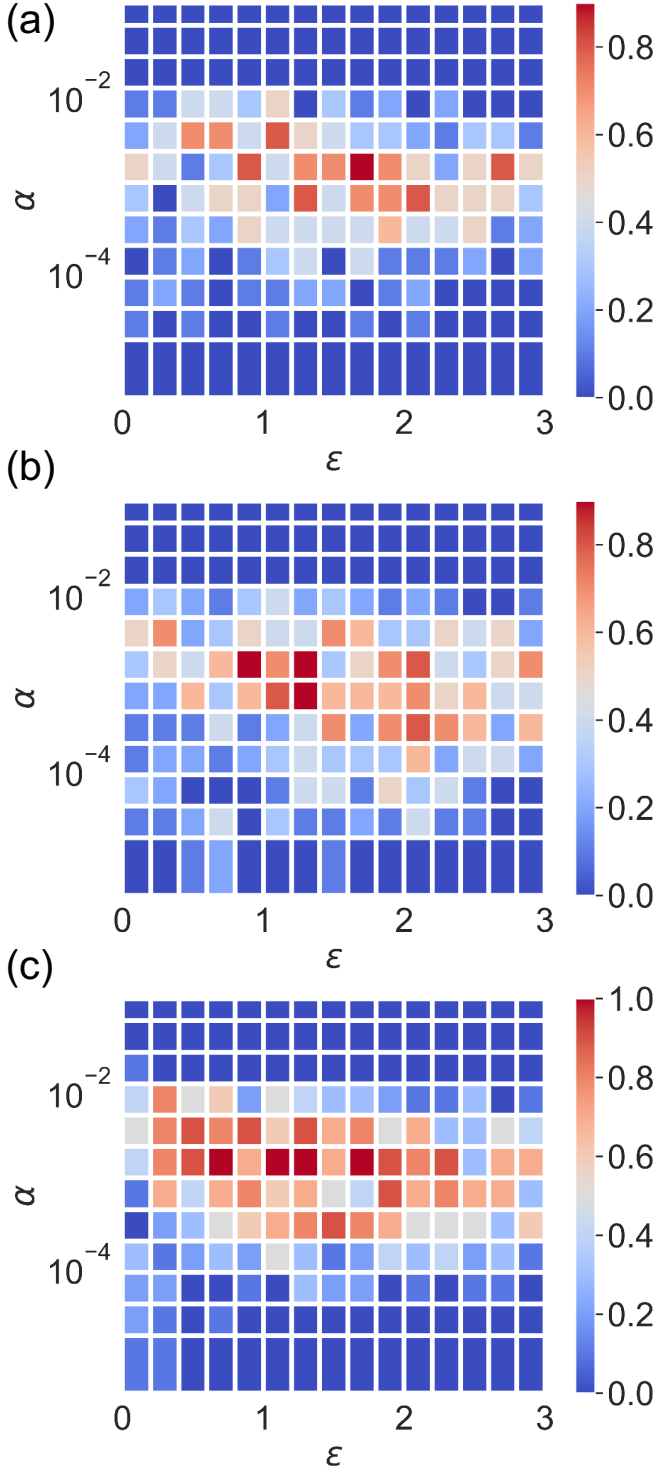


FIG. 12. Effects of hyperparameters ϵ and α on the prediction performance. (a-c) Color-coded DV values in the plane of the two hyperparameters for the Hastings-Powell, food-chain, and Lotka-Volterra systems, respectively. Each DV value is obtained using 50 statistical realizations.

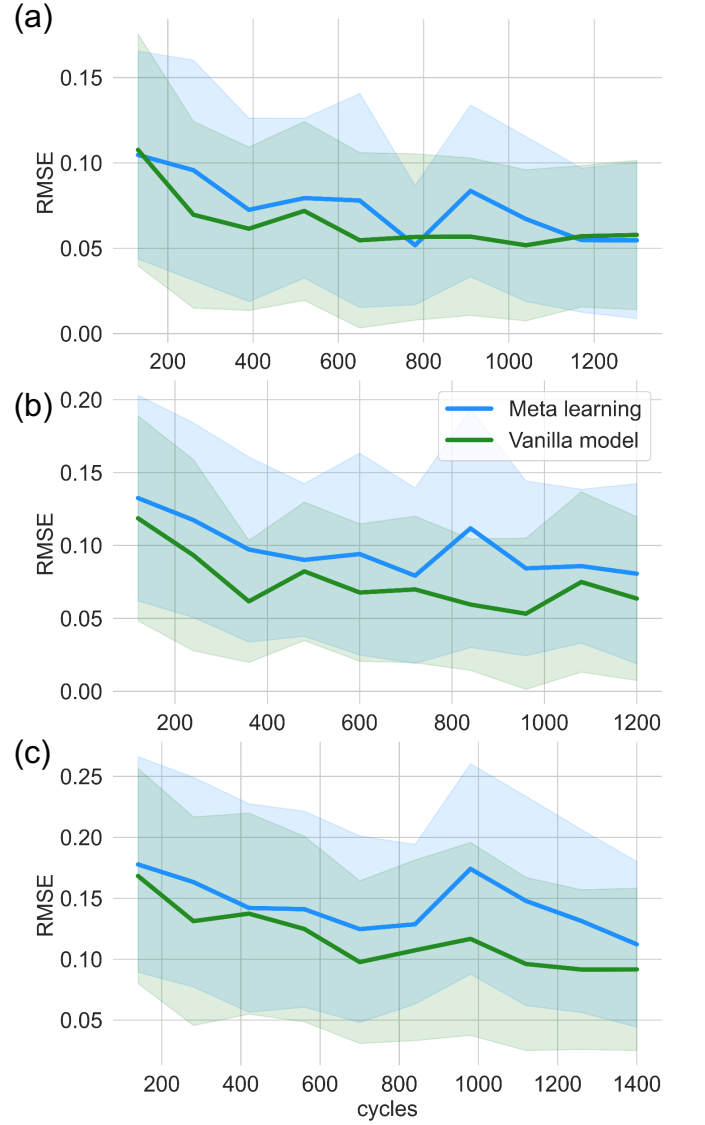


FIG. 13. Short-term prediction of ecosystems by meta-learning and standard frameworks. (a-c) RMSE versus the training length for the Hastings-Powell, chaotic food-chain, and chaotic Lotka-Volterra systems, respectively. The RMSEs and variabilities (in shade) are calculated from the ensemble of 50 independently trained machines.

mean-square error (RMSE) defined as

$$\text{RMSE}(\mathbf{y}, \hat{\mathbf{y}}) = \sqrt{\frac{1}{T_p} \frac{1}{N} [y_n(t) - \hat{y}_n(t)]^2}, \quad (\text{G1})$$

where \mathbf{y} and $\hat{\mathbf{y}}$ are the true and predicted time series, respectively, $N = 3$ is the system dimension, and T_p denotes the prediction time. Figure 13 presents results for the three ecosystems. It can be seen that meta-learning and standard frameworks exhibit similar performance, suggesting that, with respect to short-term prediction of the state evolution, meta-learning offers no apparent advantage. A plausible reason is that meta-learning re-

quires an adaptation phase during which learning is conducted based on time series from a number of synthetic chaotic systems. While exhibiting similar attractors, the

detailed dynamical evolution of these systems are quite different from that of the target ecosystem, compromising the accuracy of short-term prediction.

-
- [1] N. D. Haynes, M. C. Soriano, D. P. Rosin, I. Fischer, and D. J. Gauthier, Reservoir computing with a single time-delay autonomous Boolean node, *Phys. Rev. E* **91**, 020801 (2015).
- [2] L. Larger, A. Baylón-Fuentes, R. Martinenghi, V. S. Udaltsov, Y. K. Chembo, and M. Jacquot, High-speed photonic reservoir computing using a time-delay-based architecture: Million words per second classification, *Phys. Rev. X* **7**, 011015 (2017).
- [3] J. Pathak, Z. Lu, B. Hunt, M. Girvan, and E. Ott, Using machine learning to replicate chaotic attractors and calculate Lyapunov exponents from data, *Chaos* **27**, 121102 (2017).
- [4] Z. Lu, J. Pathak, B. Hunt, M. Girvan, R. Brockett, and E. Ott, Reservoir observers: Model-free inference of unmeasured variables in chaotic systems, *Chaos* **27**, 041102 (2017).
- [5] J. Pathak, B. Hunt, M. Girvan, Z. Lu, and E. Ott, Model-free prediction of large spatiotemporally chaotic systems from data: A reservoir computing approach, *Phys. Rev. Lett.* **120**, 024102 (2018).
- [6] T. L. Carroll, Using reservoir computers to distinguish chaotic signals, *Phys. Rev. E* **98**, 052209 (2018).
- [7] K. Nakai and Y. Saiki, Machine-learning inference of fluid variables from data using reservoir computing, *Phys. Rev. E* **98**, 023111 (2018).
- [8] Z. S. Roland and U. Parlitz, Observing spatio-temporal dynamics of excitable media using reservoir computing, *Chaos* **28**, 043118 (2018).
- [9] A. Griffith, A. Pomerance, and D. J. Gauthier, Forecasting chaotic systems with very low connectivity reservoir computers, *Chaos* **29**, 123108 (2019).
- [10] J. Jiang and Y.-C. Lai, Model-free prediction of spatiotemporal dynamical systems with recurrent neural networks: Role of network spectral radius, *Phys. Rev. Res.* **1**, 033056 (2019).
- [11] G. Tanaka, T. Yamane, J. B. Héroux, R. Nakane, N. Kanazawa, S. Takeda, H. Numata, D. Nakano, and A. Hirose, Recent advances in physical reservoir computing: A review, *Neu. Net.* **115**, 100 (2019).
- [12] H. Fan, J. Jiang, C. Zhang, X. Wang, and Y.-C. Lai, Long-term prediction of chaotic systems with machine learning, *Phys. Rev. Res.* **2**, 012080 (2020).
- [13] C. Zhang, J. Jiang, S.-X. Qu, and Y.-C. Lai, Predicting phase and sensing phase coherence in chaotic systems with machine learning, *Chaos* **30**, 083114 (2020).
- [14] C. Klos, Y. F. K. Kossio, S. Goedeke, A. Gilra, and R.-M. Memmesheimer, Dynamical learning of dynamics, *Phys. Rev. Lett.* **125**, 088103 (2020).
- [15] P. Chen, R. Liu, K. Aihara, and L. Chen, Autoreservoir computing for multistep ahead prediction based on the spatiotemporal information transformation, *Nat. Commun.* **11**, 4568 (2020).
- [16] L.-W. Kong, H.-W. Fan, C. Grebogi, and Y.-C. Lai, Machine learning prediction of critical transition and system collapse, *Phys. Rev. Res.* **3**, 013090 (2021).
- [17] D. Patel, D. Canaday, M. Girvan, A. Pomerance, and E. Ott, Using machine learning to predict statistical properties of non-stationary dynamical processes: System climate, regime transitions, and the effect of stochasticity, *Chaos* **31**, 033149 (2021).
- [18] J. Z. Kim, Z. Lu, E. Nozari, G. J. Pappas, and D. S. Bassett, Teaching recurrent neural networks to infer global temporal structure from local examples, *Nat. Machine Intell.* **3**, 316 (2021).
- [19] H. Fan, L.-W. Kong, Y.-C. Lai, and X. Wang, Anticipating synchronization with machine learning, *Phys. Rev. Res.* **3**, 023237 (2021).
- [20] L.-W. Kong, H.-W. Fan, C. Grebogi, and Y.-C. Lai, Emergence of transient chaos and intermittency in machine learning, *J. Phys. Complex.* **2**, 035014 (2021).
- [21] E. Bollt, On explaining the surprising success of reservoir computing forecaster of chaos? The universal machine learning dynamical system with contrast to VAR and DMD, *Chaos* **31**, 013108 (2021).
- [22] D. J. Gauthier, E. Bollt, A. Griffith, and W. A. Barbosa, Next generation reservoir computing, *Nat. Commun.* **12**, 1 (2021).
- [23] L.-W. Kong, Y. Weng, B. Glaz, M. Haile, and Y.-C. Lai, Reservoir computing as digital twins for nonlinear dynamical systems, *Chaos* **33**, 033111 (2023).
- [24] Z.-M. Zhai, L.-W. Kong, and Y.-C. Lai, Emergence of a resonance in machine learning, *Phys. Rev. Res.* **5**, 033127 (2023).
- [25] M. Yan, C. Huang, P. Bienstman, P. Tino, W. Lin, and J. Sun, Emerging opportunities and challenges for the future of reservoir computing, *Nat. Commun.* **15**, 2056 (2024).
- [26] Z.-M. Zhai, M. Moradi, L.-W. Kong, B. Glaz, M. Haile, and Y.-C. Lai, Model-free tracking control of complex dynamical trajectories with machine learning, *Nat. Commun.* **14**, 5698 (2023).
- [27] Z.-M. Zhai, M. Moradi, L.-W. Kong, and Y.-C. Lai, Detecting weak physical signal from noise: A machine-learning approach with applications to magnetic-anomaly-guided navigation, *Phys. Rev. Appl.* **19**, 034030 (2023).
- [28] Z.-M. Zhai, M. Moradi, B. Glaz, M. Haile, and Y.-C. Lai, Machine-learning parameter tracking with partial state observation, *Phys. Rev. Res.* **6**, 013196 (2024).
- [29] H. Jaeger, The "echo state" approach to analysing and training recurrent neural networks-with an erratum note, Bonn, Germany: German National Research Center for Information Technology GMD Technical Report **148**, 13 (2001).
- [30] W. Mass, T. Nachtschlaeger, and H. Markram, Real-time computing without stable states: A new framework for neural computation based on perturbations, *Neur. Comp.* **14**, 2531 (2002).
- [31] A. R. Rissman and S. Gillon, Where are ecology and biodiversity in social-ecological systems research? A review of research methods and applied recommendations, *Con-*

- serv. Lett. **10**, 86 (2017).
- [32] S. N. Wood, Statistical inference for noisy nonlinear ecological dynamic systems, *Nature* **466**, 1102 (2010).
- [33] S. Christin, É. Herve, and N. Lecomte, Applications for deep learning in ecology, *Methods Ecol. Evol.* **10**, 1632 (2019).
- [34] J. M. Drake, C. Randin, and A. Guisan, Modelling ecological niches with support vector machines, *J. Appl. Ecol.* **43**, 424 (2006).
- [35] D. R. Cutler, T. C. Edwards Jr, K. H. Beard, A. Cutler, K. T. Hess, J. Gibson, and J. J. Lawler, Random forests for classification in ecology, *Ecology* **88**, 2783 (2007).
- [36] W.-X. Wang, R. Yang, Y.-C. Lai, V. Kovanis, and C. Grebogi, Predicting catastrophes in nonlinear dynamical systems by compressive sensing, *Phys. Rev. Lett.* **106**, 154101 (2011).
- [37] K. Course and P. B. Nair, State estimation of a physical system with unknown governing equations, *Nature* **622**, 261 (2023).
- [38] A. Wikner, J. Harvey, M. Girvan, B. R. Hunt, A. Pomerance, T. Antonsen, and E. Ott, Stabilizing machine learning prediction of dynamics: Novel noise-inspired regularization tested with reservoir computing, *Neural Netw.* (2023).
- [39] D. Tuia, B. Kellenberger, S. Beery, B. R. Costelloe, S. Zuffi, B. Risse, A. Mathis, M. W. Mathis, F. van Langevelde, T. Burghardt, *et al.*, Perspectives in machine learning for wildlife conservation, *Nat. Commun.* **13**, 792 (2022).
- [40] M. Pichler and F. Hartig, Machine learning and deep learning—A review for ecologists, *Methods Ecol. Evol.* **14**, 994 (2023).
- [41] C. Finn, P. Abbeel, and S. Levine, Model-agnostic meta-learning for fast adaptation of deep networks, in *International Conference on Machine Learning* (PMLR, 2017) pp. 1126–1135.
- [42] T. Hospedales, A. Antoniou, P. Micaelli, and A. Storkey, Meta-learning in neural networks: A survey, *IEEE Trans. Pattern Anal. Mach. Intell.* **44**, 5149 (2021).
- [43] Y.-X. Wang, D. Ramanan, and M. Hebert, Meta-learning to detect rare objects, in *Proceedings of the IEEE/CVF International Conference on Computer Vision* (2019) pp. 9925–9934.
- [44] T. S. Talagala, R. J. Hyndman, and G. Athanasopoulos, Meta-learning how to forecast time series, *J. Forecast.* **42**, 1476 (2023).
- [45] B. N. Oreshkin, D. Carпов, N. Chapados, and Y. Bengio, Meta-learning framework with applications to zero-shot time-series forecasting, in *Proceedings of the AAAI Conference on Artificial Intelligence*, Vol. 35 (2021) pp. 9242–9250.
- [46] A. Nagabandi, I. Clavera, S. Liu, R. S. Fearing, P. Abbeel, S. Levine, and C. Finn, Learning to adapt in dynamic, real-world environments through meta-reinforcement learning, *arXiv preprint arXiv:1803.11347* (2018).
- [47] C.-D. Han, C.-Z. Wang, and Y.-C. Lai, Meta-machine-learning-based quantum scar detector, *Phys. Rev. Appl.* **19**, 064042 (2023).
- [48] M. Hermans and B. Schrauwen, Memory in linear recurrent neural networks in continuous time, *Neural Netw.* **23**, 341 (2010).
- [49] J. Z. Kim and D. S. Bassett, A neural machine code and programming framework for the reservoir computer, *Nat. Mach. Intell.* , 1 (2023).
- [50] Y. Zhang and S. P. Cornelius, Catch-22s of reservoir computing, *Phys. Rev. Res.* **5**, 033213 (2023).
- [51] A. Nichol, J. Achiam, and J. Schulman, On first-order meta-learning algorithms, *arXiv preprint arXiv:1803.02999* (2018).
- [52] A. Hastings and T. Powell, Chaos in a three-species food chain, *Ecology* **72**, 896 (1991).
- [53] K. McCann and P. Yodzis, Nonlinear dynamics and population disappearances, *Am. Nat.* **144**, 873 (1994).
- [54] J. Vano, J. Wildenberg, M. Anderson, J. Noel, and J. Sprott, Chaos in low-dimensional Lotka-Volterra models of competition, *Nonlinearity* **19**, 2391 (2006).
- [55] A. Hastings, K. C. Abbott, K. Cuddington, T. Francis, G. Gellner, Y.-C. Lai, A. Morozov, S. Petrovskii, K. Scranton, and M. L. Zeeman, Transient phenomena in ecology, *Science* **361**, eaat6412 (2018).
- [56] S. R. Proulx, D. E. Promislow, and P. C. Phillips, Network thinking in ecology and evolution, *Trends Ecol. Evol.* **20**, 345 (2005).
- [57] M. Kot, *Elements of Mathematical Ecology* (Cambridge University Press, 2001).
- [58] J. Terborgh and J. A. Estes, *Trophic Cascades: Predators, Prey, and the Changing Dynamics of Nature* (Island press, 2013).
- [59] G. Vissio, Weather-like forcing in population mortality rates (2023).
- [60] S. W. McDonald and A. N. Kaufman, Spectrum and eigenfunctions for a Hamiltonian with stochastic trajectories, *Phys. Rev. Lett.* **42**, 1189 (1979).
- [61] E. J. Heller, Bound-state eigenfunctions of classically chaotic Hamiltonian systems: scars of periodic orbits, *Phys. Rev. Lett.* **53**, 1515 (1984).
- [62] H. Xu, L. Huang, Y.-C. Lai, and C. Grebogi, Chiral scars in chaotic Dirac fermion systems, *Phys. Rev. Lett.* **110**, 064102 (2013).
- [63] J. Gu, Y. Wang, Y. Chen, K. Cho, and V. O. Li, Meta-learning for low-resource neural machine translation, *arXiv preprint arXiv:1808.08437* (2018).
- [64] S. Bouali, A novel strange attractor with a stretched loop, *Nonlinear Dyn.* **70**, 2375 (2012).
- [65] T. Matsumoto, A chaotic attractor from Chua’s circuit, *IEEE Trans. Circuits Syst.* **31**, 1055 (1984).
- [66] S. Dadras and H. R. Momeni, A novel three-dimensional autonomous chaotic system generating two, three and four-scroll attractors, *Phys. Lett. A* **373**, 3637 (2009).
- [67] Z. Wang, Y. Sun, B. J. van Wyk, G. Qi, and M. A. van Wyk, A 3-D four-wing attractor and its analysis, *Braz. J. Phys.* **39**, 547 (2009).
- [68] E. N. Lorenz, Deterministic nonperiodic flow, *J. Atmos. Sci.* **20**, 130 (1963).
- [69] J. Llibre and M. Messias, Global dynamics of the rikitake system, *Phys. D: Nonlinear Phenom.* **238**, 241 (2009).
- [70] O. E. Rössler, An equation for continuous chaos, *Phys. Lett. A* **57**, 397 (1976).
- [71] J. C. Sprott, Some simple chaotic flows, *Phys. Rev. E* **50**, R647 (1994).